

1 **Characterization of secondary organic aerosol from heated-**
2 **cooking oil emissions: evolution in composition and volatility**

3 Manpreet Takhar¹, Yunchun Li², Arthur W. H. Chan¹

4 ¹Department of Chemical Engineering and Applied Chemistry, University of Toronto, Toronto, M5S 3E5, Canada

5 ²College of Science, Sichuan Agricultural University, Ya'an, 625014, China

6 *Correspondence to:* Arthur W. H. Chan (arthurwh.chan@utoronto.ca)

7

8

9

10

11

12

13

14

15

16

17

18

19

20

21

22

23

24

25

26

27

28

29

30 **Table S1:** Description of the experiments conducted in this study.

Exp.	Canola oil SOA ($\mu\text{g m}^{-3}$)	OH exposure (molecules cm^{-3} s)	Photochemical age (h) ^a
1	26.57±2.32	5.77×10^{10}	10.7
2	75.67±5.33	6.43×10^{10}	11.9
3	93.48±13.1	7.07×10^{10}	13.1
4	151.46±12.45	8.01×10^{10}	14.8
5	108.74±17.6	8.60×10^{10}	15.9
6	207.2±11.91	9.23×10^{10}	17.1
7	2670.4±170.85	2.20×10^{11}	40.7

31 a: calculated by assuming an average atmospheric OH concentration of 1.5×10^6 molecules cm^{-3} (Mao et al., 2009).

32

33 **Table S2:** List of all the model compounds used in this study to recreate 73 along with its $f_{\text{M-15/73}}$. SIMPOL.1 (Pankow
34 and Asher, 2008) vapor pressure and its corresponding saturation concentrations are also listed for the compounds
35 quantified in this study.

#	Carbon #	Molecular weight (MW)	Derivatized MW (M)	M-15	$f_{\text{M-15/73}}$ (NIST)	$f_{\text{M-15/73}}$ (MS detector response)	Vapor pressure (atm)	Saturation concentration ($\mu\text{g m}^{-3}$)
2-COOH								
1	3	104	248	233	0.147	0.128±0.03	3.5E-07	29.5
2	4	118	262	247	0.24	0.273±0.06	1.3E-07	3.2 ^a
3	5	132	276	261	0.67	0.254±0.1	4.9E-08	54.8 ^a
4	6	146	290	275	0.198	0.143±0.04	1.9E-08	0.8 ^a
5	7	160	304	289	0.187	0.198±0.07	7.0E-09	4.2 ^a
6	8	174	318	303	0.147	0.182±0.08	2.6E-09	0.09 ^a
7	9	188	332	317	0.268	0.313±0.22	9.9E-10	0.5 ^a
2-COOH + 1-OH								
8	3	120	336	321	0.029	0.062±0.014	2.3E-09	0.19
9	4	134	350	335	0.067	0.051±0.03	8.6E-10	0.02
10	5	148	364	349	0.146	0.141±0.05	3.2E-10	0.36
11	6	162	378	363	0.106 ^{a1}	0.072±0.03	1.2E-10	5.3E-03
12	6	162	378	363	0.178 ^{a2}	0.272±0.11	1.2E-10	5.3E-03
13	7	176	392	377	0.012	0.034±0.02	4.6E-11	2.7E-02

14	8	190	406	391	0.002	n/a	6.5E-12	6.4E-04
15	9	204	420	405	n/a	n/a	2.4E-12	3.2E-03
1-COOH + 2-OH								
16	3	106	322	307	0.04	0.058±0.01	4.9E-08	400.2
17	4	120	336	321	0.116	0.052±0.04	1.8E-08	150.6
18	5	134	350	335	n/a	n/a	6.9E-09	56.7
19	6	148	364	349	n/a	0.125±0.05	2.6E-09	21.3
20	7	162	378	363	n/a	0.019±0.01	9.8E-10	8.02
21	7	162	378	363	n/a	0.026±0.01	9.8E-10	8.02
22	7	162	378	363	n/a	0.068±0.01	9.8E-10	8.02
23	7	162	378	363	n/a	0.056±0.01	9.8E-10	8.02
24	8	176	392	377	n/a	0.023±0.02	3.7E-10	3.01
25	8	176	392	377	n/a	0.026±0.01	3.7E-10	3.01
26	9	190	406	391	n/a	0.033±0.02	1.4E-10	1.1
27	9	190	406	391	n/a	0.021±0.02	1.4E-10	1.1
2-COOH + 2-OH								
28	4	150	438	423	0.07	0.029±0.002	5.7E-12	1.4E-04
29	5	164	452	437	0.059	0.057±0.01	2.1E-12	2.4E-03
30	6	178	466	451	0.05	n/a	8.0E-13	3.5E-05
1-COOH + 1-OH								
31	2	76	220	205	0.123	0.11±0.01	1.9E-05	162375.7
32	3	90	234	219	0.479	0.48±0.15	7.5E-06	61085.0
33	4	104	248	233	0.024 ^{b1}	0.053±0.02	2.8E-06	22979.9
34	4	104	248	233	0.226 ^{b2}	0.099±0.05	2.8E-06	22979.9
35	4	104	248	233	0.179 ^{b3}	0.147±0.06	2.8E-06	22979.9
36	5	118	262	247	0.043 ^{c1}	0.034±0.01	1.1E-06	8644.9
37	5	118	262	247	0.06 ^{c2}	0.064±0.01	1.1E-06	8644.9
38	5	118	262	247	0.341 ^{c3}	0.245±0.12	1.1E-06	8644.9
39	6	132	276	261	0.04 ^{d1}	0.043±0.01	3.9E-07	3252.2
40	6	132	276	261	0.089 ^{d2}	0.068±0.02	3.9E-07	3252.2
41	6	132	276	261	0.215 ^{d3}	0.106±0.06	3.9E-07	3252.2

42	7	146	290	275	0.06	0.071±0.01	1.5E-07	1223.5
43	8	160	304	289	0.109	0.05±0.008	5.6E-08	460.3
44	9	174	318	303	0.074	n/a	2.1E-08	173.1
1-COOH								
45	6	116	188	173	0.69	0.604±0.05	6.1E-05	5.7
46	7	130	202	187	1.18	0.656±0.02	2.3E-05	5.3
47	8	144	216	201	1.14	0.769±0.06	8.6E-06	4.8
48	9	158	230	215	1.24	0.815±0.04	3.2E-06	4.4
49	10	172	244	229	1.02	0.947±0.11	1.2E-06	3.9

36 a: Bilde et al. (2003).

37 a1: positional isomers

38 a2: positional isomers

39 b1: α -hydroxyisobutyric acid

40 b2: β -hydroxybutyric acid

41 b3: 3-hydroxybutyric acid

42 c1: α -hydroxyvaleric acid

43 c2: β -hydroxy-n-valeric acid

44 c3: 4-hydroxyvaleric acid

45 d1: 4-methyl 2-keto pentanoic acid

46 d2: 3-hydroxycaproic acid

47 d3: 5-hydroxyhexanoic acid

48

49

50 **Table S3:** List of all the model compounds used in this study to recreate 73 for single precursor oxidation experiments
 51 along with corresponding product molar yields.

M-15	Heptanal + OH	2-heptenal + OH	2-octenal + OH	2,4-heptadienal + OH
OH exposure (molec cm⁻³ s)^a	7.71×10^{10}	6.2×10^{10}	6.02×10^{10}	5.34×10^{10}
OH reaction rate constant (cm³ molec⁻¹ s⁻¹)	3.0×10^{-11b}	4.4×10^{-11c}	4.1×10^{-11d}	4.6×10^{-10e}
1-COOH + 1-OH				
205	1.87E-07	7.38E-05	4.44E-05	9.40E-05
219	6.85E-08	1.26E-05	1.29E-05	3.84E-06
233	3.67E-06	2.97E-05	2.45E-05	2.66E-05
247	4.49E-06	5.82E-05	5.03E-05	3.77E-05
261	3.73E-06	4.78E-05	2.22E-05	0
275	6.69E-06	4.35E-06	6.46E-06	0

289	0	5.70E-07	2.27E-05	0
303	0	0	0	0
317	0	0	0	0
2-COOH				
233	1.96E-06	5.32E-06	9.26E-06	7.44E-06
247	5.56E-06	2.35E-05	3.02E-05	1.98E-05
261	1.82E-05	7.85E-05	9.24E-05	5.26E-05
275	2.87E-06	5.00E-06	3.62E-06	5.20E-06
289	3.19E-06	9.94E-07	1.34E-05	0
303	0	0	0	0
317	0	0	0	0
2-COOH + 1-OH				
321	0	0	0	0
335	3.11E-06	0	0	2.96E-05
349	1.33E-05	3.02E-05	4.20E-05	2.61E-05
363	2.29E-05	1.80E-05	7.28E-05	0
377	1.63E-06	1.38E-06	1.72E-05	1.45E-05
391	0	0	0.00016	0
2-COOH + 2-OH				
423	0	1.69E-06	1.90E-06	3.81E-06
437	0	2.15E-06	2.73E-06	5.97E-07
451	0	2.93E-06	0	9.19E-07
1-COOH + 2-OH				
307	3.41E-07	3.32E-06	0	1.06E-05
321	4.27E-06	3.82E-05	2.31E-05	0
335	0	0	0	0
349	5.50E-06	0	6.69E-05	0
363	0	4.42E-05	2.68E-05	4.86E-06
377	0	0	0	0
391	0	0	0	0
1-COOH				

173	3.70E-06	0	4.53E-05	0
187	0	1.65E-06	2.64E-06	1.73E-06
201	0	0	1.05E-06	0
215	0	0	0	0

52 a: as calculated from the decay of cyclopentane in each set of experiment.
 53 b: Atkinson and Arey (2003).
 54 c: Davis et al. (2007).
 55 d: Gao et al. (2009).
 56 e: calculated by multiplying 2-heptenal OH reaction rate constant by a factor of 105 as obtained from Kwok &
 57 Atkinson (1995).

58

59

60 Section 1. Chemical characterization using TD-GC/MS

61 Gas-phase analysis: Tenax tubes were desorbed in the thermal desorption system (TDS) for thermal desorption with
 62 initial temperature at 50 °C held for 2 minutes followed by a ramp of 60 °C min⁻¹ to 320 °C and held for 4 minutes.
 63 The analytes were transferred to the cooling injection system (CIS4, Gerstel) via a transfer line maintained at 300 °C
 64 during the run. The CIS4 was embedded with quartz wool filled quartz liner maintained at -40 °C during thermal
 65 desorption, and was heated to 320 °C at 12 °C s⁻¹, and held for 5 minutes at 320 °C. The GC column was held for 2
 66 minutes at 40 °C and heated to 250 °C at a rate of 7 °C min⁻¹ and held for additional 5 minutes at 250 °C.

67 Particle-phase analysis: 4 mm diameter filter punches were inserted into glass tubes (6 mm OD × 178 mm length,
 68 Gerstel) and placed in the TDS for thermal desorption. The temperature ramping program for thermal desorption was
 69 from 40 °C initial temperature held for 2 minutes followed by a ramp of 60 °C min⁻¹ to 320 °C and held for 5 minutes
 70 at 320 °C. After the analytes were desorbed in the TDS, they were transferred to the cooling injection system (CIS4,
 71 Gerstel) via a transfer line maintained at 300 °C during the run. The CIS4 was embedded with quartz wool filled quartz
 72 liner maintained at 10 °C during thermal desorption to preconcentrate the desorbed analytes. The CIS was heated from
 73 10 °C to 320 °C at 12 °C s⁻¹, and held for an additional 7 minutes at 320 °C. The GC column was heated from 40 °C
 74 to 300 °C at a ramp of 10 °C min⁻¹ and held for 5 minutes at 300 °C. All samples were analyzed under electron impact
 75 at 70 eV using a standard tungsten filament with a source temperature at 230 °C. The MS was operated at 3.1 scans s⁻¹
 76 with an acquisition range from mass-to-charge (*m/z*) ratio 35 to 500.

77

78 Section 2. Procedure to recreate *m/z* 73

79 **Step 1:** Extract all model M-15 ions from the total ion chromatogram.

80 **Step 2:** Divide each M-15 ion with its corresponding $f_{M-15,73}$. Wherever, NIST $f_{M-15,73}$ was not available, $f_{M-15,73}$
 81 was calculated from the instrument detector response.

82 **Step 3:** Since higher m/z ions are susceptible to fragmentation under high electron ionization efficiency (70 eV in our
83 study), therefore caution must be taken in recreating M-15 ions so as to avoid double counting of actual (or real) peaks.
84 An example of this scenario is shown in Fig. S4 (a), using an example chromatogram of m/z 233, 335 and 349. As
85 shown in Fig. S4 (a), m/z 233 has large number of fragments from higher m/z ions, and some of these fragments belong
86 to actual m/z . Peaks at retention time (RT) = 13.059 min corresponds to m/z 335 while at RT = 14.599 min belongs to
87 m/z 349. Therefore, in order not to overestimate these peaks, fragments of higher m/z should be set to zero when
88 recreating smaller m/z .

89 **Step 4:** Repeat step 3 iteratively for remaining M-15 ions to minimize the effect of double counting, and only
90 accounting for signal from actual or real peaks as shown in Fig. S4 (b).

91 **Step 5:** Add all M-15 together to recreate 73 as shown in Fig. S4 (c).

92

93 **Section 3. Sample calculation for Sect. 3.3.1 (formation of particle-phase oxidation products)**

94 Estimation of SOA formation potential using product yields of VOC precursor oxidation products were done as
95 follows:

96 M-15 ion = 219 corresponds to 3-hydroxypropanoic acid has a yield of 1.26E-05 upon photooxidation of 2-heptenal
97 which is used to estimate SOA formation for canola oil photooxidation using Eq. (4) in main text.

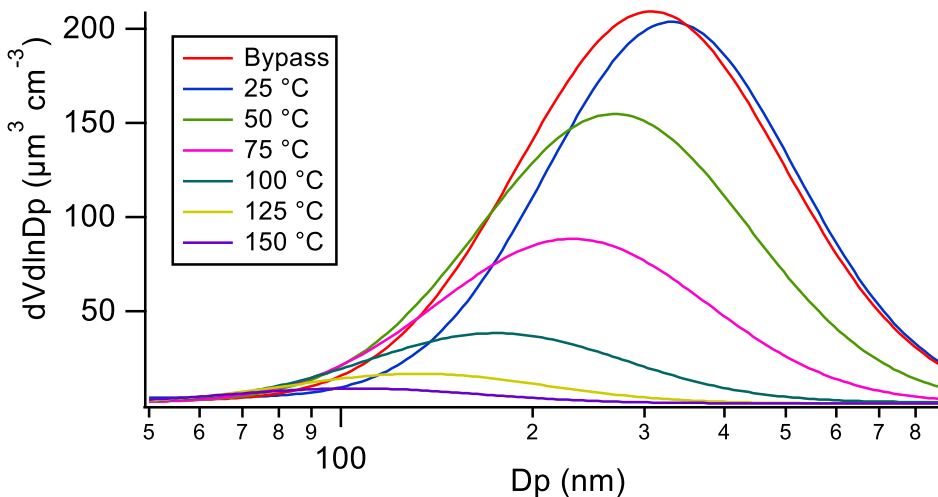
98 Where, γ_{ij} represents yields of products (i) from photooxidation of 2-heptenal (j) (obtained from Table S3), and ΔVOC_j
99 represents the decay in concentration of 2-heptenal during photooxidation of canola oil vapors, and was calculated
100 based on the measured OH exposure.

101 Therefore, for 3-hydroxypropanoic acid (or M-15 = 219) the SOA formation can be predicted as:

$$102 \quad SOA_{pred} = 1.26E - 05 * 299 * 90 = 0.339 \mu\text{g m}^{-3}.$$

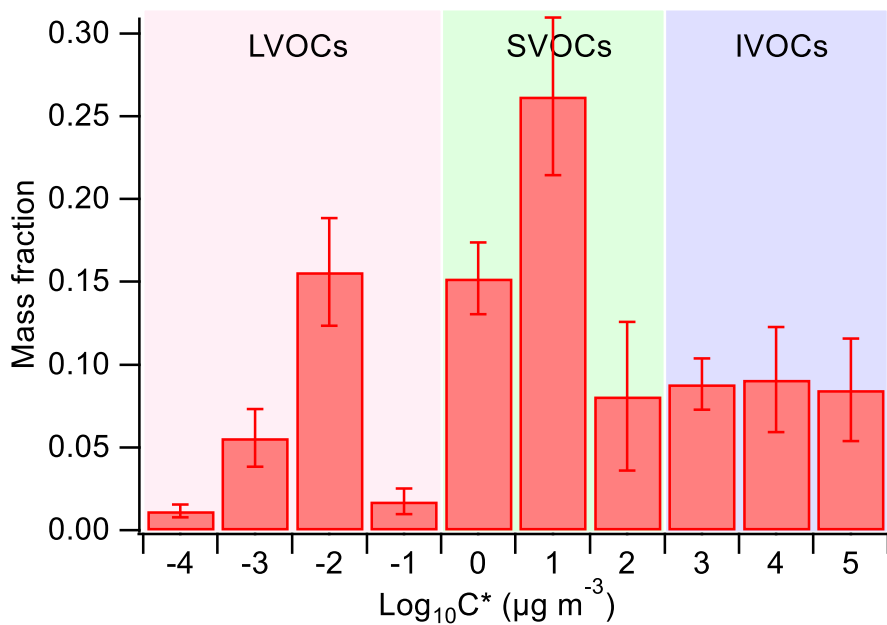
103 Similarly, using above methodology SOA formation can be estimated from other VOC precursors such as heptanal,
104 2-octenal, and 2,4-heptadienal.

105



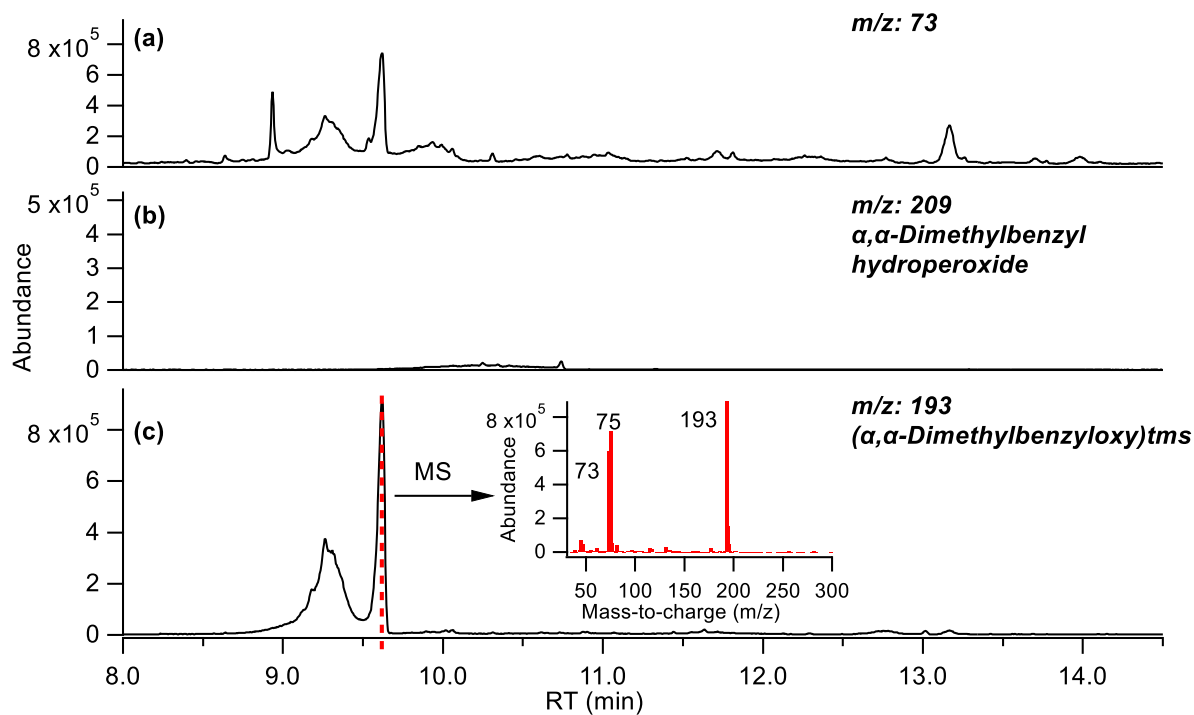
106
 107 **Figure S1.** Particle volume distribution of canola oil SOA at an OH exposure of 9.23×10^{10} molecules cm^{-3} s measured by SMPS
 108 when subject to heating in a thermodenuder. The volume mode diameter shifts from 332 nm at 25 °C to 106 nm at 150 °C
 109 corresponding to a decrease in volume concentration of ~96%.

110

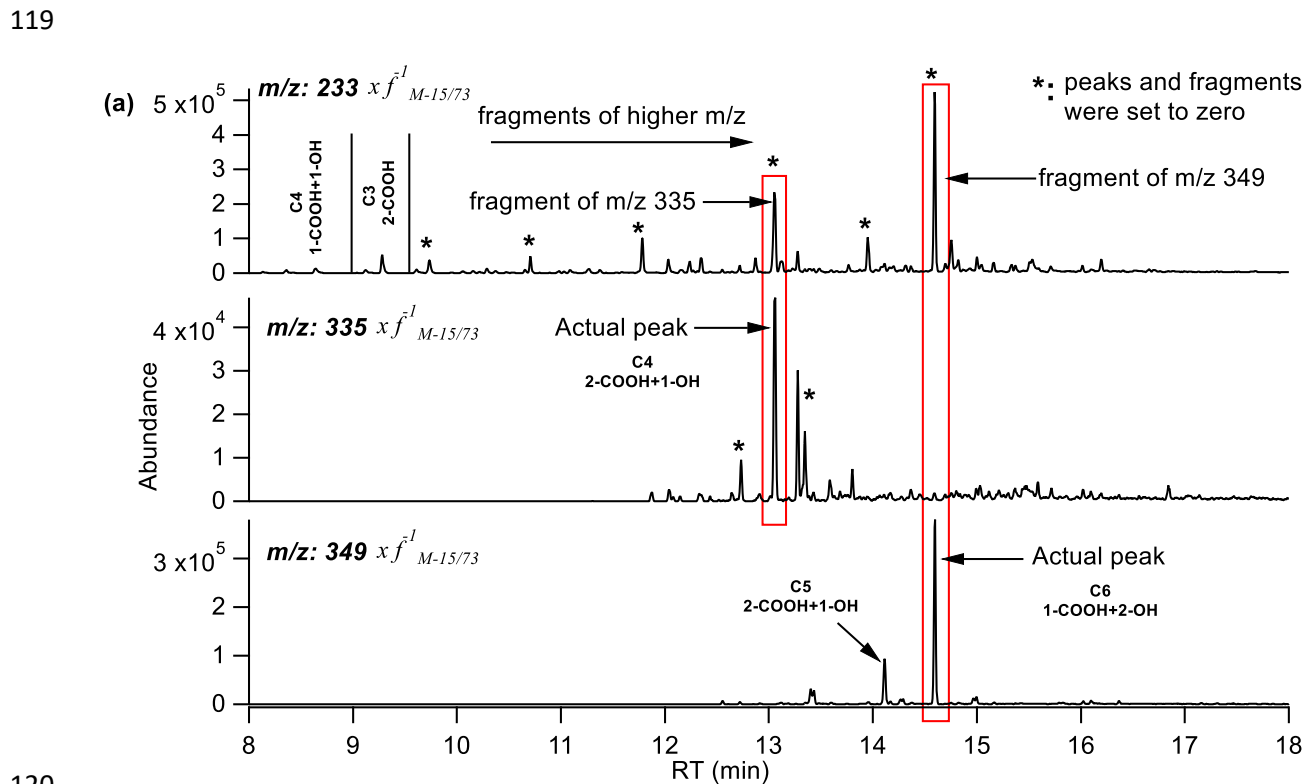


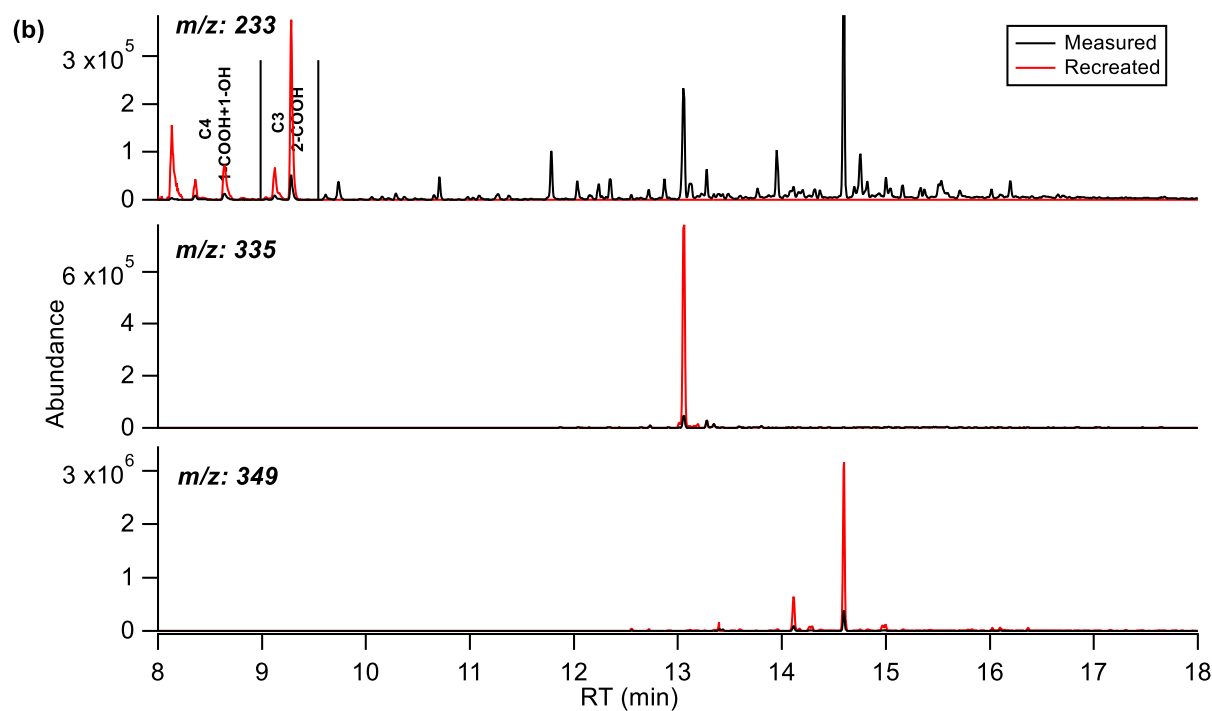
111
 112 **Figure S2.** Volatility distribution of canola oil SOA at an OH exposure of 9.23×10^{10} molecules cm^{-3} s. The volatility distribution
 113 corresponds to 24% mass in LVOCs, ~50% in SVOCs, and 26% in IVOCs. The error bars represent $\pm 1\sigma$.

114

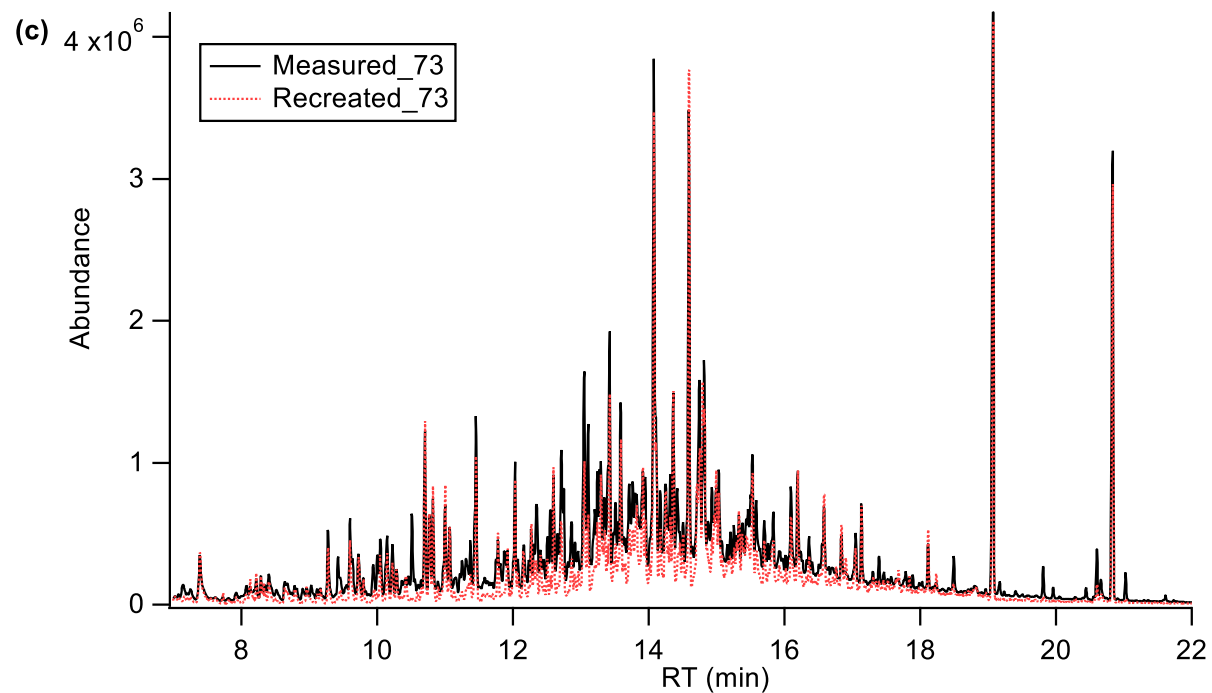


115
 116 **Figure S3.** Chromatogram of cumene hydroperoxide upon *in situ* derivatization (a). Based on the analytical technique discussed in
 117 main text, extracted M-15 ($m/z = 209$) chromatogram of cumene hydroperoxide contains no peaks as shown in panel (b), instead
 118 the derivatized form of R-OH is observed as shown in panel (c) along with its mass spectrum shown in the inset.





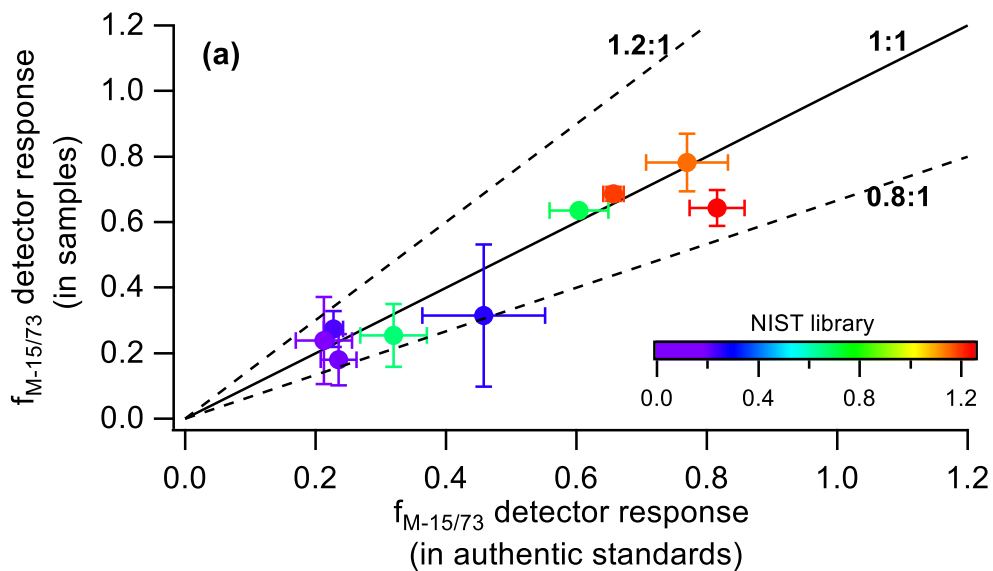
121



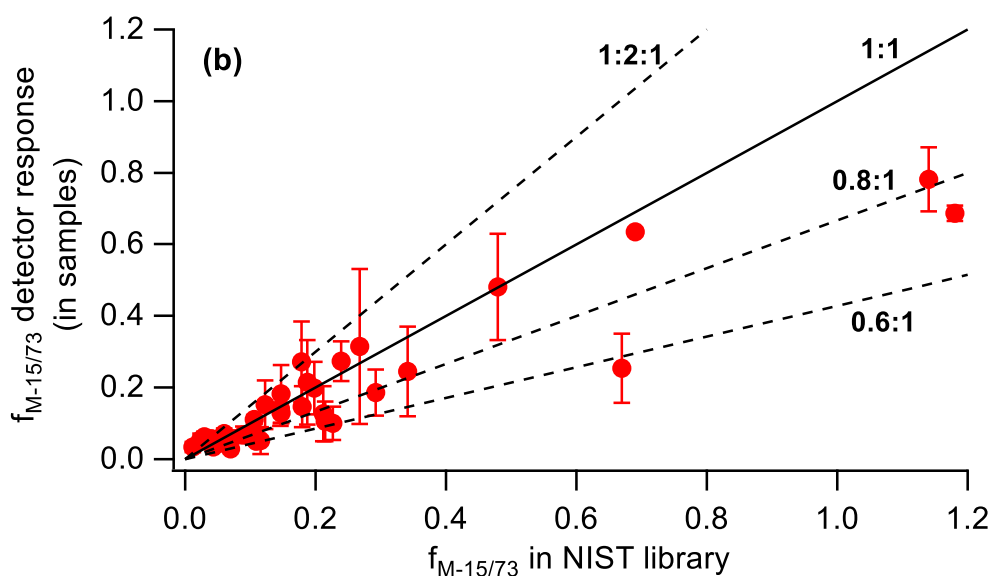
122

123 **Figure S4.** Illustration to recreate m/z 73. (a) shows the unprocessed M-15 chromatograms obtained from canola oil photooxidation
 124 highlighting that lower m/z ions are susceptible to interference from higher m/z , therefore appropriate processing (refer to Sect. 2,
 125 step 3) of chromatograms should be carried out to account for these interferences. (b) chromatograms obtained after cleaning of
 126 fragments from each model m/z . (c) total ion chromatogram of measured and recreated 73.

127



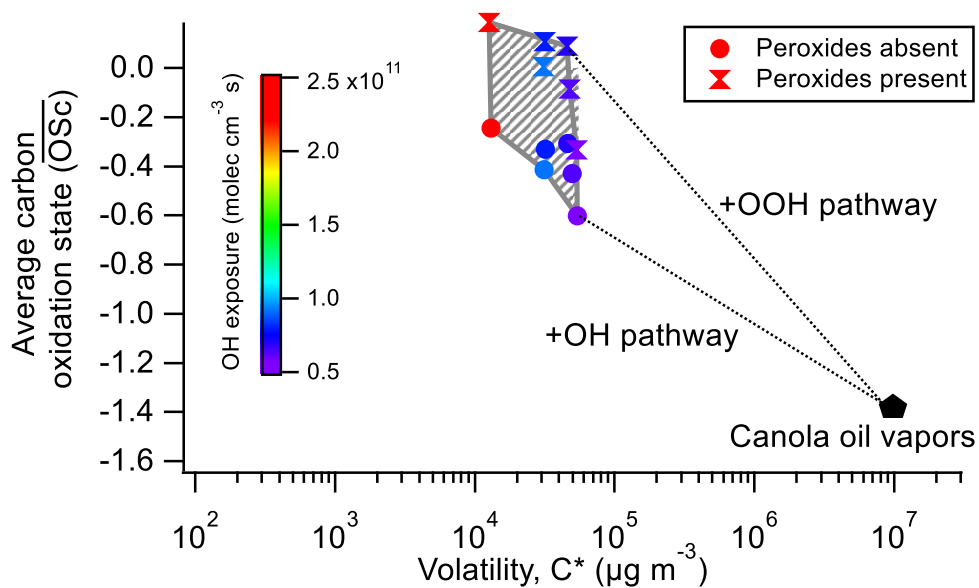
128



129

130 **Figure S5.** Calculated uncertainties in pseudo molecular ion fraction of model components. (a) compares $f_{M-15/73}$ from instrument
131 detector response in samples vs that in authentic standards colour coded with $f_{M-15/73}$ available in NIST library. (b) shows the
132 comparison of $f_{M-15/73}$ obtained from instrument detector response to that available in NIST library. Both comparisons show that
133 the uncertainty in measurement of $f_{M-15/73}$ is within 20% for measured compounds except for tartaric acid which is within 40%
134 uncertainty.

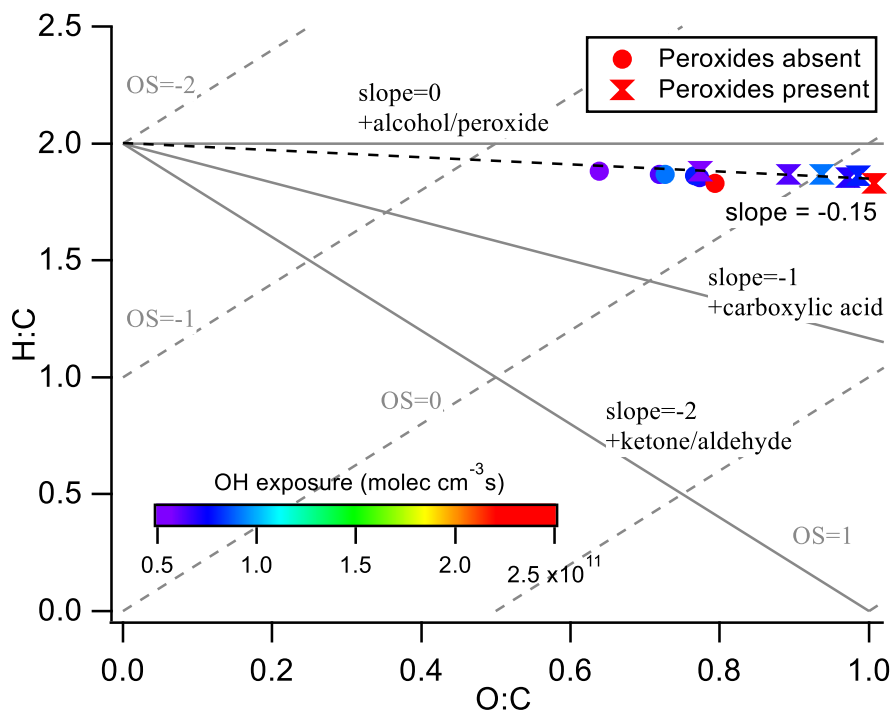
135



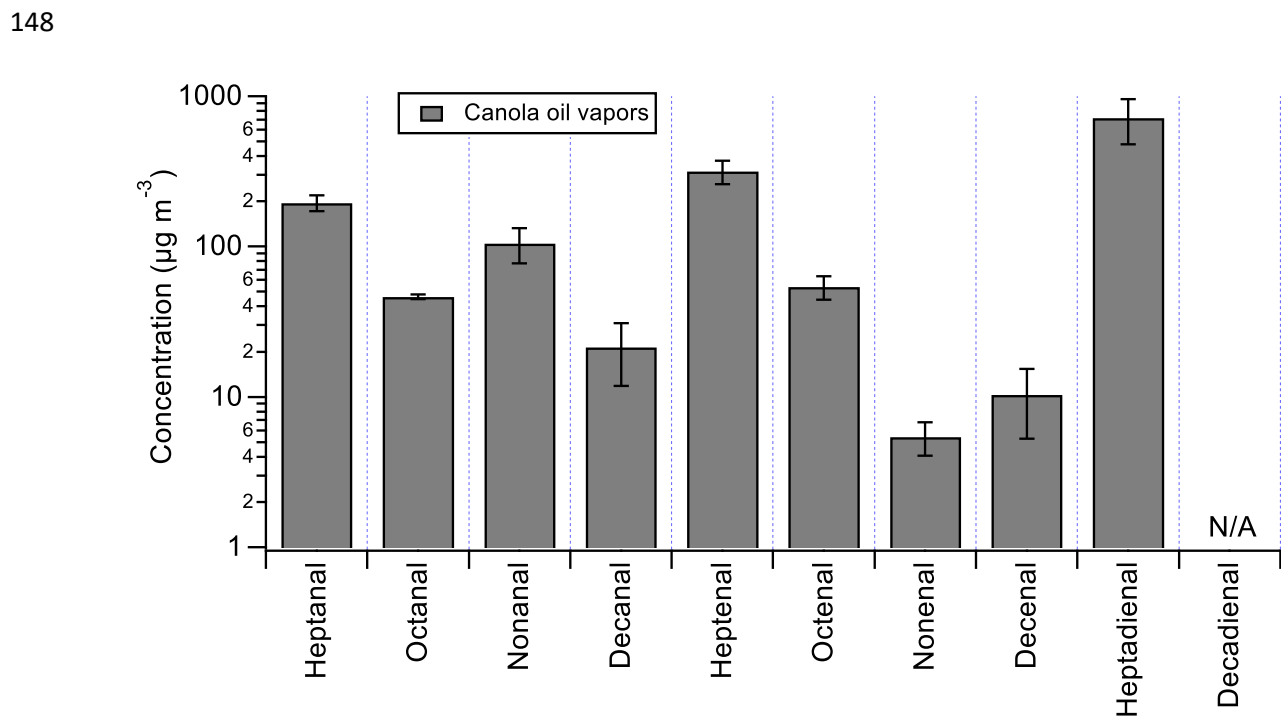
136

137 **Figure S6.** 2D-VBS for canola oil SOA upon photochemical aging in the atmosphere. The coloured markers represent bulk
 138 volatility of SOA under different photochemical aging conditions, while the black marker represents properties of canola oil vapors
 139 before oxidation. The shaded area corresponds to formation of SOA products with the uncertainty associated in identifying hydroxyl
 140 and peroxide groups. If all hydroxyl groups were instead classified as peroxide groups, the \overline{OSc} increases but the bulk volatility of
 141 SOA shows a minor decrease suggesting that classification of peroxide groups as hydroxyl groups has little effect on estimation of
 142 volatility.

143

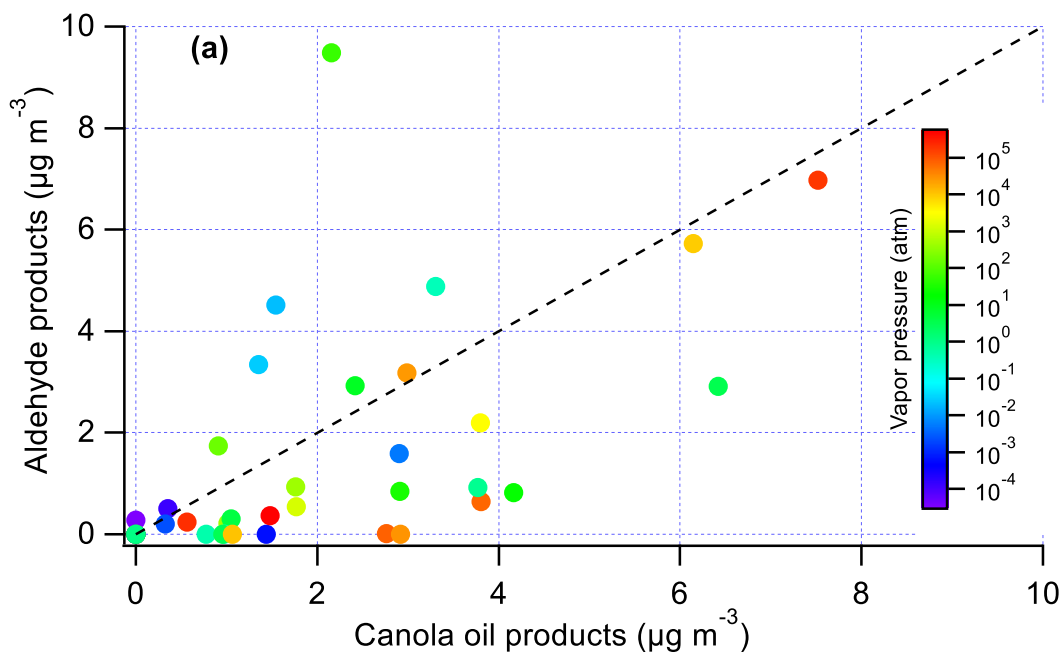


144
 145 **Figure S7.** Van Krevelen diagram of canola oil SOA coloured by different OH exposure considering the presence of peroxides.
 146 The slope of -0.15 is observed when the formation of peroxides is considered in canola oil SOA similar to that of no-peroxides
 147 assumption (Fig. 4, main text).

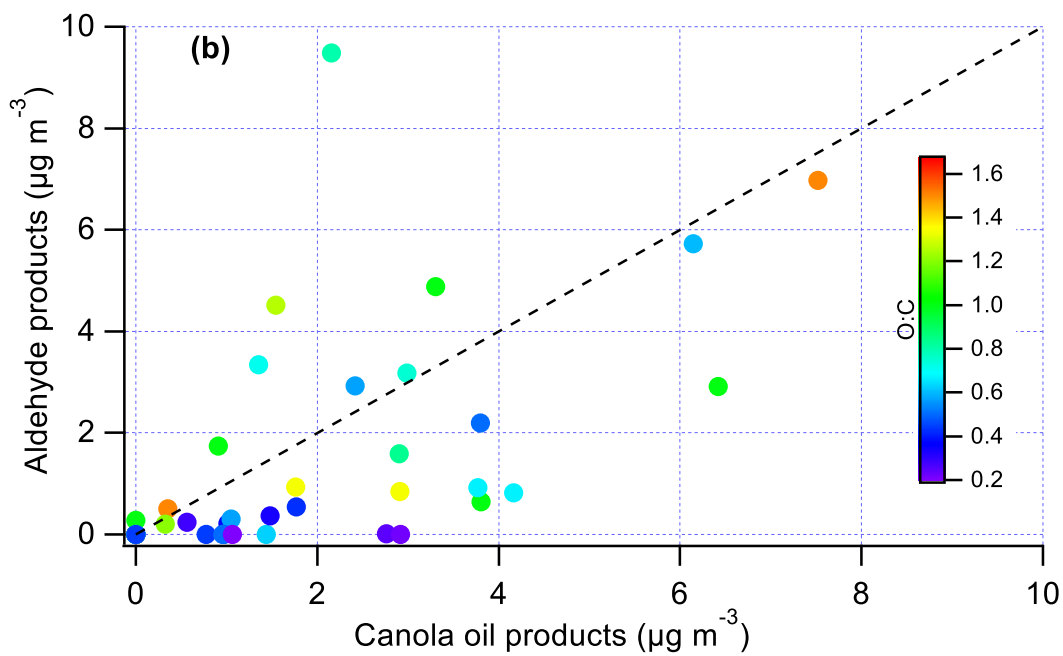


149
 150 **Figure S8.** Concentration of different aldehydes quantified in this study.

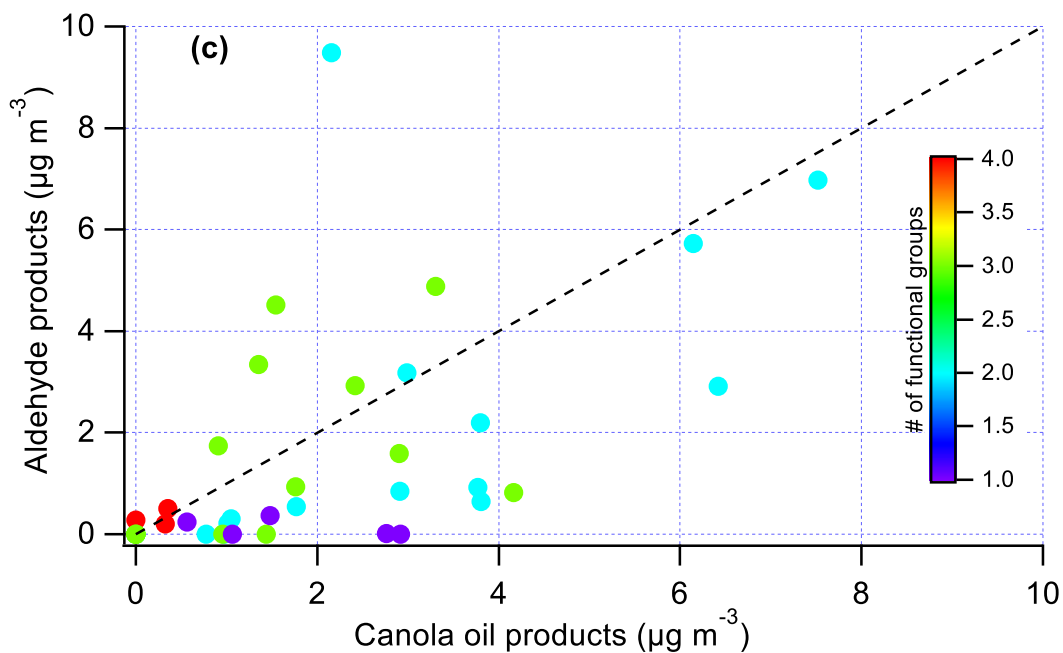
151



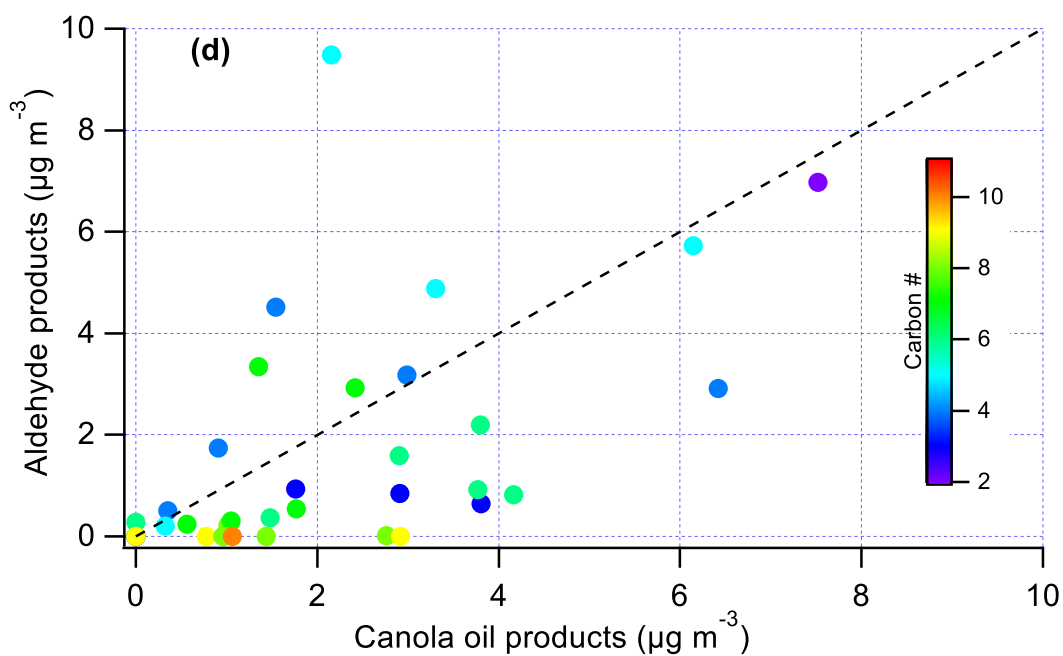
152



153



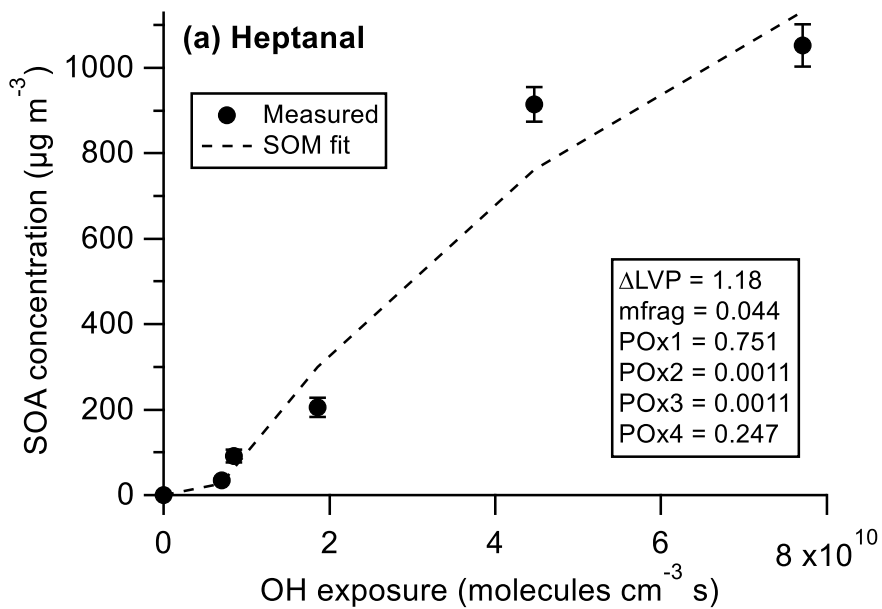
154



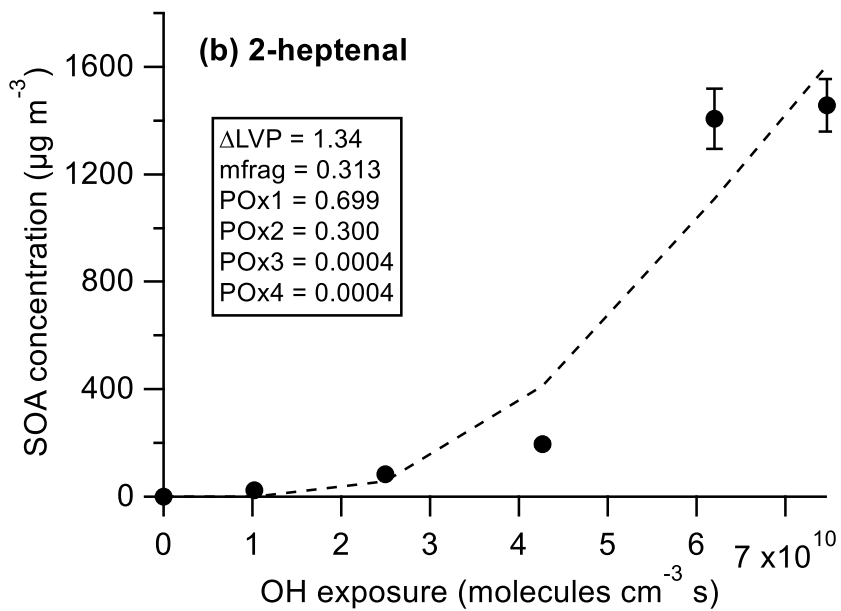
155

156 **Figure S9.** Comparison of GC measured products from canola oil photooxidation and aldehydes photooxidation by vapor pressure
 157 (a), O/C ratios (b), # of functional groups (c), and carbon # (d). In general, aldehydes SOA products are underestimated for lower
 158 O/C ratios and number of functional groups, suggesting that canola oil SOA favors partitioning of more oxygenated compounds
 159 than SOA formed from aldehydes.

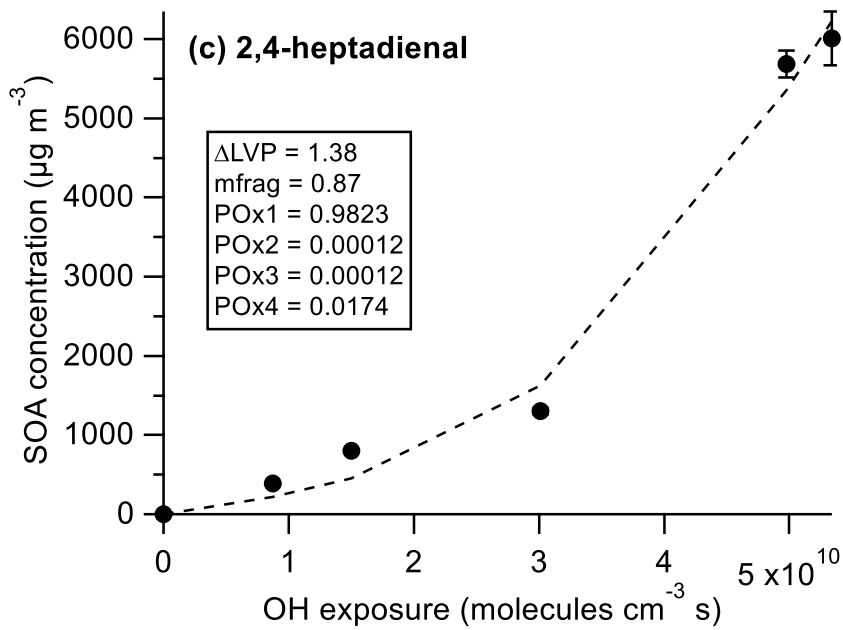
160



161



162



163

164 **Figure S10.** Estimation of SOM parameters by fitting SOA concentrations against OH exposure for heptanal (a), *trans*-2-heptenal

165 (b), and *trans,trans*-2,4-heptadienal (c) photooxidation.

166

167 **References**

- 168 Atkinson, R. and Arey, J.: Atmospheric Degradation of Volatile Organic Compounds, *Chem. Rev.*, 103(12), 4605–
169 4638, doi:10.1021/cr0206420, 2003.
- 170 Bilde, M., Svenningsson, B., Mønster, J. and Rosenørn, T.: Even-odd alternation of evaporation rates and vapor
171 pressures of C3-C9 dicarboxylic acid aerosols, *Environ. Sci. Technol.*, 37(7), 1371–1378, doi:10.1021/es0201810,
172 2003.
- 173 Davis, M. E., Gilles, M. K., Ravishankara, A. R. and Burkholder, J. B.: Rate coefficients for the reaction of OH with
174 (E)-2-pentenal, (E)-2-hexenal, and (E)-2-heptenal, *Phys. Chem. Chem. Phys.*, 9(18), 2240–2248,
175 doi:10.1039/b700235a, 2007.
- 176 Gao, T., Andino, J. M., Rivera, C. C. and Marquez, M. F.: Rate Constants of the Gas-Phase Reactions of OH
177 Radicals with trans-2-Hexenal, trans-2-Octenal, and trans-2-Nonenal, *Int. J. Chem. Kinet.*, 41(7), 483–489,
178 doi:10.1002/kin, 2009.
- 179 Kwok, E. S. C. and Atkinson, R.: Estimation of hydroxyl radical reaction rate constants for gas-phase organic
180 compounds using a structure-reactivity relationship: An update, *Atmos. Environ.*, 29(14), 1685–1695,
181 doi:10.1016/1352-2310(95)00069-B, 1995.
- 182 Mao, J., Ren, X., Brune, W. H., Olson, J. R., Crawford, J. H., Fried, A., Huey, L. G., Cohen, R. C., Heikes, B.,
183 Singh, H. B., Blake, D. R., Sachse, G. W., Diskin, G. S., Hall, S. R. and Shetter, R. E.: Airborne measurement of
184 OH reactivity during INTEX-B, *Atmos. Chem. Phys.*, 9(1), 163–173, doi:10.5194/acp-9-163-2009, 2009.
- 185 Pankow, J. F. and Asher, W. E.: SIMPOL.1: A simple group contribution method for predicting vapor pressures and
186 enthalpies of vaporization of multifunctional organic compounds, *Atmos. Chem. Phys.*, 8(10), 2773–2796,
187 doi:10.5194/acp-8-2773-2008, 2008.

188